Genetics and Molecular Research

Roles of osteocyte apoptosis in steroid-induced avascular necrosis of the femoral head

R. Bai[1]*, W. Feng[2]*, W.L. Liu[1], Z.H.Q. Zhao[1], A.Q. Zhao[1], Y. Wang[1], W.X. Wang[1], L. Sun[1], L.S.H. Wu[1] and S.H.X. Cui[1]

[1]Department of Pediatric Orthopedics,
The Second Affiliated Hospital of Inner Mongolia Medical University, Hohhot, China
[2]Department of Orthopedics,
The Second Affiliated Hospital of Inner Mongolia Medical University, Hohhot, China

*These authors contributed equally to this study.
Corresponding authors: W.L. Liu / Z.H.Q. Zhao
E-mail: liuwanlinnmg@sohu.com / nmgjpxh@163.com

Genet. Mol. Res. 15 (1): gmr.15017529
Received December 16, 2015
Accepted January 15, 2016
Published March 18, 2016
DOI http://dx.doi.org/10.4238/gmr.15017529

ABSTRACT. An animal model of steroid-induced avascular necrosis of the femoral head (SANFH) was established to investigate the roles of osteocyte apoptosis in this process. Forty five-month-old male and female Japanese white rabbits were randomly divided into groups A (hormone + endotoxin), B (hormone alone), C (endotoxin alone), and D (blank control). Animals were sacrificed two and four weeks following the final treatment (N = 5 for each group at each time point). Bilateral femoral heads were fixed and decalcified, and empty lacunae were counted by hematoxylin staining. At weeks 2 and 4, the empty lacunae percentage was significantly higher in group A than that in groups B, C, or D ($P < 0.01$), while no significant difference was observed between these latter three. At week 2, all osteocyte apoptosis indexes were within normal ranges in all the groups, which therefore did not significantly differ in this respect ($P > 0.05$). However, at week 4, the apoptotic index was significantly higher in group A than that in

groups B, C, or D ($P < 0.01$), comparisons between which revealed no such differences. Moreover, a positive correlation was observed between the percentage of empty lacunae and the apoptotic index at week 4 in group A ($r = 0.893$). We conclude that osteocyte apoptosis plays an important role in SANFH.

Key words: Hormone; Femoral head; Necrosis; Apoptosis

INTRODUCTION

Since the 1960s, many researchers have been investigating the pathogenesis of steroid-induced avascular necrosis of the femoral head (SANFH), and thus many different mechanisms have been proposed, including fat metabolism disorders, increased intraosseous pressure, osteoporosis, hormone cytotoxicity, intravascular coagulation, potential vasculitis and vascular injury, and pro-coagulation (Nishida et al., 2008; Takano-Murakami et al., 2009). However, many questions remain concerning the pathological changes to osteocytes and osteoblasts in early SANFH and their potential causes, especially the manner in which the death of such cells is brought about and the reversible factors involved. In recent years, preliminary investigations have been performed on the role of osteocyte and osteoblast apoptosis in SANFH (Kerachian et al., 2009; Yun et al., 2009), providing a new understanding of the pathogenesis of this disease. Unfortunately, none of these studies have extensively examined the mechanism responsible for apoptosis in these two cell types. What are the pathological changes occurring in the bone marrow hematopoietic cells, an important component of the femoral head, in early SANFH? These issues are the focus of the present study.

SANFH was induced in rabbits, which were subsequently sacrificed (N = 5 for each group at each time point) two and four weeks following administration of the final treatment. Bilateral femoral heads were then fixed and decalcified, and empty lacunae were counted by hematoxylin (H&E) staining. Morphologic changes in osteocytes were observed using an electron microscope, and their apoptosis was detected by terminal deoxynucleotidyl transferase-mediated deoxyuridine triphosphate nick-end labeling (TUNEL). The relationship between SANFH and osteocyte apoptosis was clarified, in order to provide slightly informal for further investigation into the pathogenesis of this condition.

MATERIAL AND METHODS

Experimental materials

Experimental animals

Forty healthy adult male and female Japanese white rabbits (provided by Beijing Fuhao Animal Breeding Center, Beijing, China), each weighing 2.5 ± 0.5 kg and receiving a standard diet, were raised solitarily in individual cages. The animals were certified by the National Institute of Medical Experiments of China (certificate No. 20090137).

Experimental instruments

The following were provided by the Molecular Biology Research Center and Electron Microscopy Center of Inner Mongolia Medical College: electron microscope (H-700H; Hitachi,

Tokyo, Japan), ultramicrotome (2800; LKB, Bromma, Sweden), image analysis system (JD801; Xircom, Jiangsu, China), ultrapure water purifier (Merck Millipore, Billerica, MA, USA), microscope (Olympus CX31, Tokyo, Japan).

Reagents

The following reagents were used in our experiments: *Escherichia coli* endotoxin (provided by National Institutes for Food and Drug Control, Beijing, China), methylprednisolone (Pharmacia & Upjohn, Puurs, Belgium), monoclonal antibody N45.1 oxidative DNA damage detection kit (Sigma-Aldrich, Tokyo, Japan), TUNEL apoptosis detection kit (Roche, Basel, Switzerland). H&E stain, ethylenediaminetetraacetic acid (EDTA) decalcifying solution, and other conventional reagents were provided by the Molecular Biology Research Center of Inner Mongolia Medical College.

Experimental methods

Animal grouping and drug administration

Experimental animals were randomly divided into four groups (N = 10 for each group) using a random number table. Group A, the model group, received two intravenous injections of *E. coli* endotoxin (100 μg/kg) at an interval of 24 h. The second injection was followed by three intramuscular injections of methylprednisolone (20 mg/kg), also at intervals of 24 h. Control Group B received two intravenous injections of *E. coli* endotoxin as above, after which, three intramuscular injections of normal saline (20 mg/kg) were administered at intervals of 24 h. Control Group C received two intravenous injections of normal saline at an interval of 24 h, followed by three intramuscular injections of methylprednisolone (20 mg/kg) at 24-h intervals. Control Group D was given two intravenous injections of normal saline at an interval of 24 h. This was followed by a further three intramuscular injections of normal saline (20 mg/kg), also separated by intervals of 24 h. Animals were sacrificed (N = 5 for each group at each time point) by air embolism two and four weeks after the final injection. Bilateral femoral heads were then obtained from animals under relatively sterile conditions.

Preparation of specimens

One side of the excised femoral heads was fixed with 5% glutaraldehyde for one week, and the other with 10% formaldehyde solution. All femoral heads were then decalcified with 15% EDTA for 45 days, and embedded in paraffin.

Histological examination by light microscopy

To observe histopathological changes, 4-μm sections of paraffin-embedded tissues were observed using H&E staining and light microscopy (Olympus CX31, Tokyo, Japan) at 100 and 400X magnification. Pathological changes relating to osteocyte necrosis were expressed as the percentage of empty lacunae. Specifically, 50 lacunae were examined in each of five high-power fields at 100X magnification, and the numbers of empty lacunae in each field were counted to determine a percentage. The empty lacunae percentage in femoral subchondral bone has been widely adopted as a histological criterion for diagnosis of SANFH. Values greater than 8-12% in such tissue, the normal range in adult rabbits, indicate bone necrosis.

Transmission electron microscopy

A bone block of 1 x 1 x 1 mm was harvested 0.2-0.3 cm below the cartilage of the 5% glutaraldehyde-fixed femoral head, decalcified with 5% nitric acid for 2-3 h, fixed with 1% osmium tetroxide for 1 h, dehydrated with an alcohol gradient, and embedded in Epon 812 (Heidebio, Co., Beijing, China). Successive solutions of 1:1, 2:1, and 3:1 embedding medium: absolute ethyl alcohol were used. After embedding, the bone blocks were incubated at 37°C for 24 h, polymerized in a 60°C oven for 48 h, sliced into 50-nm sections using an ultramicrotome, and stained with uranyl acetate and lead citrate. The ultrathin sections were then observed under an electron microscope.

Detection of osteocyte apoptosis by TUNEL

Osteocyte apoptosis was detected following the TUNEL kit manufacturer protocol, as follows: a) For specimen pretreatment, prepared paraffin tissue sections were placed in a staining jar, washed twice with xylene and absolute ethyl alcohol, washed once each with 95 and 75% ethanol, washed with phosphate-buffered saline (PBS) for 5 min, hydrolyzed with proteinase K solution (20 µg/mL) at room temperature for 15 min, and washed four times with distilled water after removal of tissue proteins. b) In the staining jar, sections were washed twice with PBS containing 2% hydrogen peroxide. c) Immediately following removal of excess liquid with filter paper, sections were incubated with two drops of terminal transferase (TdT) buffer. d) TdT enzyme reaction solution (54 µL) was then incubated with samples after removal of excess liquid with filter paper. e) In a staining jar, sections were washed and the reaction terminated with buffers preheated to 37°C, at which temperature the samples were kept. f) After three washes with PBS, specimens were directly incubated with two drops of peroxidase-labeled anti-digoxigenin antibody. g) Four PBS washes were then carried out. h) Sections were directly incubated with freshly prepared 0.05% 3,3'-diaminobenzidine. i) Four washes with distilled water were then performed. j) Specimens were counterstained with methyl green at room temperature, washed three times with distilled water, then washed three times with 100% *n*-butanol using the same method. Finally, sections were dehydrated three times with xylene, mounted, dried, and observed under a light microscope (Olympus CX31, Tokyo, Japan), using which, images were recorded. The nuclei of TUNEL-positive cells appeared brown or brownish yellow, and occasionally, positive granules were observed within the cytoplasm. Fifty osteocytes were counted in each of five high-power fields for each section. The apoptotic index was calculated as the number of apoptotic cells / total number of cells in the field.

Statistical analysis

All data are reported as means ± SD and were analyzed in SPSS 13.0 (SPSS Inc., Chicago, IL, USA). Statistical tests relating to the empty lacunae percentage and osteocyte apoptosis index were performed using analysis of variance. Pairwise comparisons between sample means were performed using the least significant difference test. The relationship between empty lacunae percentage and apoptosis rate in group A was assessed using linear correlation. A linear relationship between the two variables is indicated by $-1 \leq r \leq +1$. Positive and negative *r*-values signify positive and negative correlations, respectively. $P < 0.05$ was considered to represent statistical significance.

RESULTS

Histological examination

Visual inspection revealed no significant difference in gross morphology of the exposed femoral head between the four groups.

Changes observed by light microscopy

In the week-2 group A, necrosis, mostly subchondral, was observed in the histopathological sections of femoral head; porosity, thinning, and disordered arrangement of trabecular bone, a decreased number of hematopoietic cells, an increased number of empty lacunae, an increase in fat cell size in the bone marrow, and fusion of some fat cells into bubbles were also observed (Figure 1). In group B, regularly arranged, intact, compact, and full trabecular bone containing clearly visible osteocytes with large, centrally located nuclei; abundant hematopoietic cells and relatively few fat cells, both with normal morphology, in the bone marrow (Figure 2). In group C, no necrosis; regularly arranged and intact trabecular bone containing clearly visible osteocytes (Figure 3). In group D, regularly arranged, intact, compact, and full trabecular bone containing clearly visible osteocytes with large, centrally located nuclei; abundant hematopoietic cells and relatively normal fat cells (each cell consists of a peripheral rim of cytoplasm, in which the nucleus is embedded surrounding a single large central globule of fat), both with normal morphology, in bone marrow (Figure 4). In week-4 group A, typical necrosis; porosity, thinning, disordered arrangement, and even breakage of trabecular bone, with visible fragments; a decreased number of hematopoietic cells; irregular arrangement of osteoblasts; a significantly increased number of empty lacunae; an increase in fat cell size in bone marrow, and fusion of some fat cells into bubbles (Figure 5). In group B, regularly arranged, intact, compact and full trabecular bone containing clearly visible osteocytes with large, centrally located nuclei; abundant hematopoietic cells and relatively few fat cells, both with normal morphology, in bone marrow (Figure 6). In group C, no necrosis; regularly arranged and intact trabecular bone (Figure 7). In group D, regularly arranged, intact, compact, and full trabecular bone containing clearly visible osteocytes with large, centrally located nuclei; abundant hematopoietic cells with normal morphology in bone marrow (Figure 8). The average percentages of empty lacunae for each group at weeks 2 and 4 are reported in Table 1.

Figure 1. At week 2, empty lacunae were seen in the tissue from group A (400X magnification).

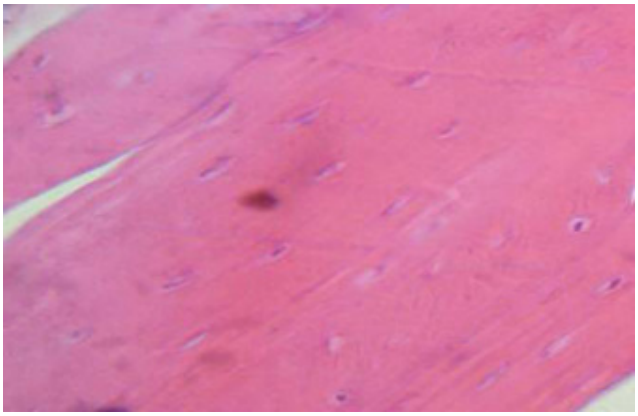

Figure 2. At week 2, clearly visible osteocytes were observed in lacunae from group B specimens (400X magnification).

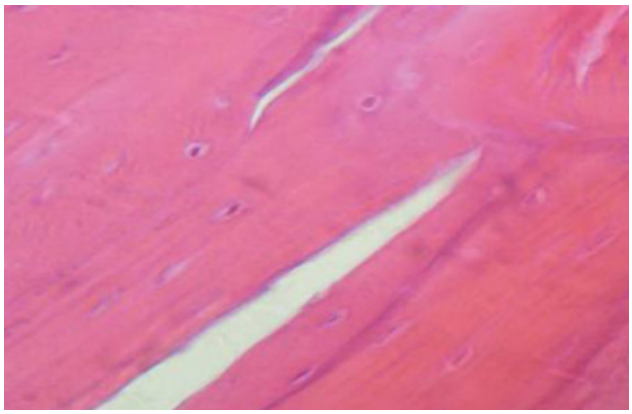

Figure 3. At week 2, clearly visible osteocytes were observed in lacunae from group C specimens (400X magnification).

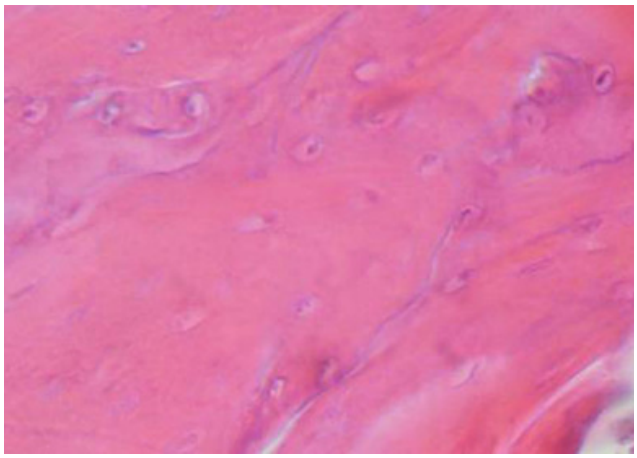

Figure 4. At week 2, clearly visible osteocytes were observed in lacunae from group D specimens (400X magnification).

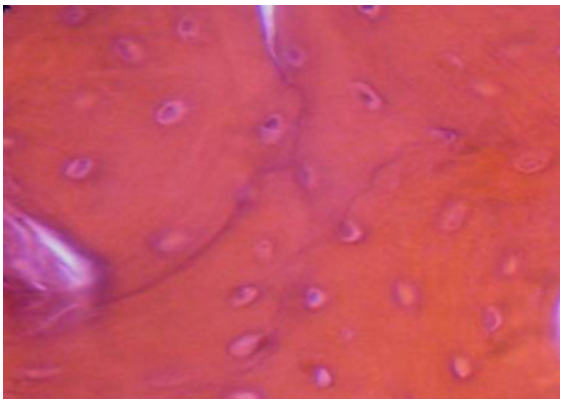

Figure 5. At week 4, a large number of empty lacunae were present in the tissue from group A (400X magnification).

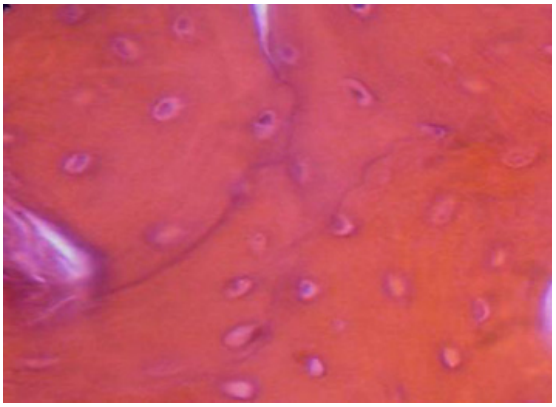

Figure 6. At week 4, clearly visible osteocytes were observed in lacunae from group B specimens (400X magnification).

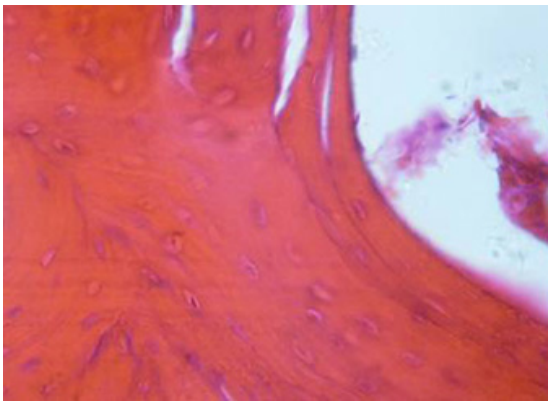

Figure 7. At week 4, clearly visible osteocytes were observed in lacunae from group B specimens (400X magnification).

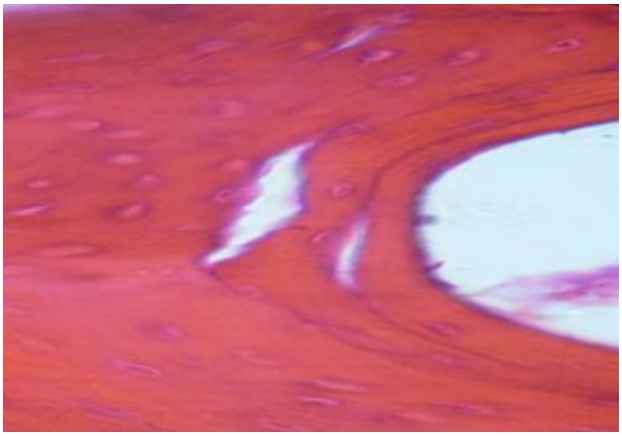

Figure 8. At week 4, clearly visible osteocytes were observed in lacunae from group D specimens (400X magnification).

Table 1. Average empty lacunae rate at weeks 2 and 4 (%).

Group	Week 2	Week 4
A	16.200 ± 0.583	30.2 ± 1.050
B	8.800 ± 0.352	12.0 ± 1.207
C	8.200 ± 0.459	11.4 ± 1.076
D	8.800 ± 0.572	11.4 ± 1.253

The empty lacunae percentage was significantly higher in group A than in groups B, C, or D at weeks 2 (F = 46.775, P = 0.00) and 4 (F = 83.915, P = 0.00), but no significant difference was found between the latter three groups.

Changes observed by electron microscopy

In week-2 group A, karyopyknosis in osteocytes, chromatin margination, protrusions, mitochondrial vacuoles, large numbers of lysosomes and secretory granules in the cytoplasm, and bone marrow bleeding were observed. In groups B, C, and D, osteocytes and bone marrow hematopoietic cells showed normal ultrastructure. In week-4 group A, loss of membrane integrity, karyopyknosis, chromatin margination, apoptotic bodies, and disappearance of organelles were observed. In groups B, C, and D, osteocytes and bone marrow hematopoietic cells demonstrated normal ultrastructure (Figures 9-12).

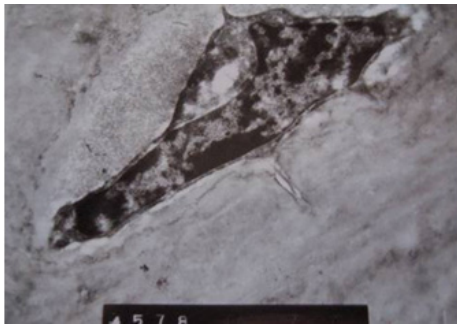

Figure 9. Week-2 group A: Karyopyknosis in osteocytes, chromatin margination, protrusions, mitochondrial vacuoles, and large numbers of lysosomes and secretory granules were observed in the cytoplasm (10,000X magnification).

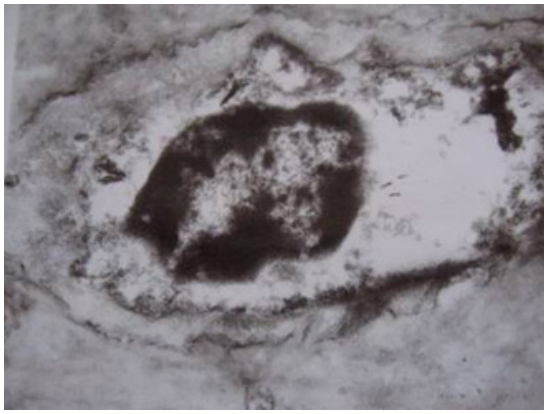

Figure 10. Week-4 group A: Loss of membrane integrity, karyopyknosis, chromatin margination, disappearance of organelles, and apoptotic bodies were observed. (12,000X magnification).

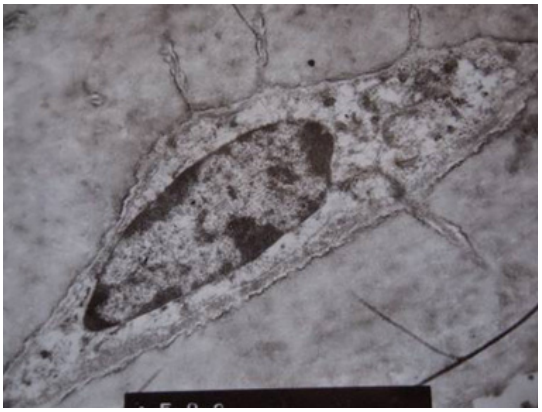

Figure 11. Week-4 group A: Karyopyknosis of osteocytes, chromatin margination, protrusions, mitochondrial vacuoles, and large numbers of lysosomes and secretory granules were observed in the cytoplasm (10,000X magnification).

Figure 12. Week-4 group D: Osteocytes and bone marrow hematopoietic cells demonstrated normal ultrastructure (10,000X magnification).

Detection of osteocyte apoptosis by TUNEL

The normal apoptotic index for healthy Japanese white rabbits is 2-3%. At week 2, osteocyte apoptosis indexes were 2.20 ± 0.47, 2.00 ± 0.53, 2.20 ± 0.37, and 1.60 ± 0.47 in groups A, B, C, and D, respectively. Therefore, all were within the normal range, and no significant difference was found between the four groups ($P > 0.05$; Figures 13-16; SPSS data analysis). At week 4, bone specimens from group A contained positive cells with brown particles in their nuclei, and a large number of apoptotic cells had appeared in the bone marrow tissue. The apoptotic index was significantly higher in group A than in groups B, C, or D ($P < 0.01$), while there was no significant difference between these latter three groups in this regard. Apoptosis indexes of 32.40 ± 1.24, 2.40 ± 1.92, 1.80 ± 0.77, and 2.10 ± 0.95 were measured in groups A, B, C, and D, respectively ($F = 140.30$, $P = 0.00$; Figures 17-20; SPSS data analysis).

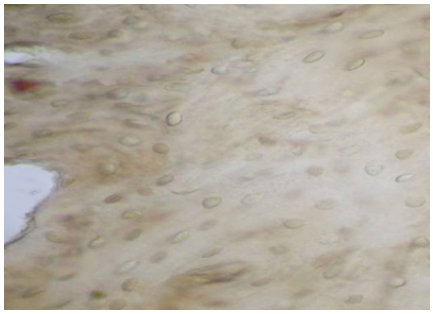

Figure 13. At week 2, no apoptotic cells were seen in the tissue from group A (400X magnification).

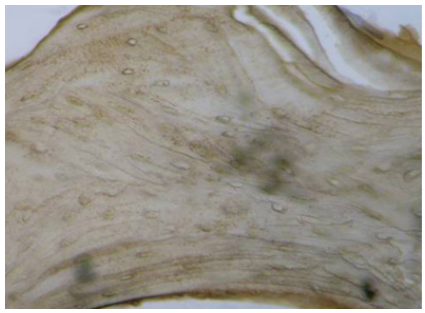

Figure 14. At week 2, no apoptotic cells were seen in the tissue from group B (400X magnification).

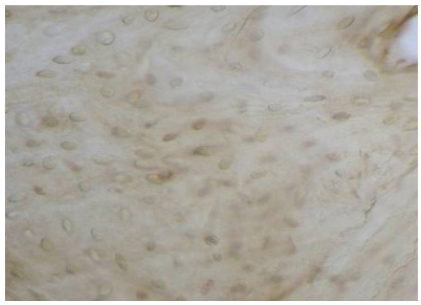

Figure 15. At week 2, no apoptotic cells were seen in the tissue from group C (400X magnification).

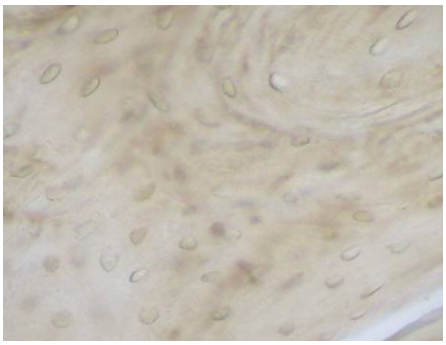

Figure 16. At week 2, no apoptotic cells were seen in the tissue from group D (400X magnification).

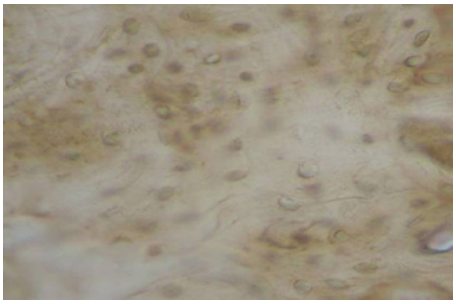

Figure 17. At week 4, a large number of apoptotic cells were observed in group A specimens (400X magnification).

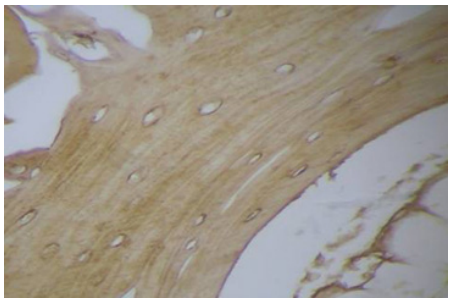

Figure 18. At week 4, no apoptotic cells were seen in the tissue from group B (400X magnification).

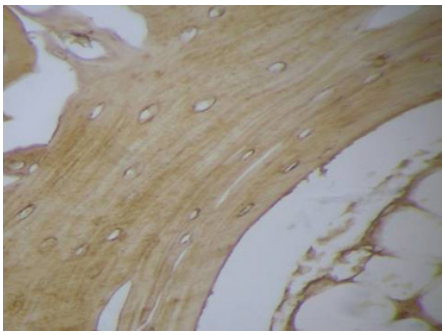

Figure 19. At week 4, no apoptotic cells were seen in the tissue from group C (400X magnification).

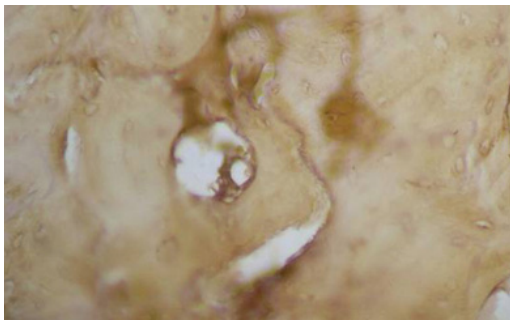

Figure 20. At week 4, no apoptotic cells were seen in the tissue from group D (400X magnification).

A positive correlation was ascertained between the percentage of empty lacunae and the osteocyte apoptosis rate in group A at week 4 (r = 0.893; Table 2).

Table 2. Empty lacunae percentage and osteocyte apoptosis rate in group A at week 4.

	Animal number				
	1	2	3	4	5
Empty lacunae percentage	28	32	27	35	29
Osteocyte apoptosis rate	24	27	20	41	29

DISCUSSION

Animal modeling

Avascular necrosis of the femoral head induced by long- or short-term intensive use of adrenocortical hormone has attracted wide attention in the medical profession. The number of reported clinical cases has been increasing since the first report of SANFH by Pietrograndi (1955). It chiefly affects young and middle-aged people, and is bilateral in most cases, affecting a large area of tissue. This condition is considerably more severe than idiopathic avascular necrosis, resulting in high disability rates. Interestingly, in 2009 (Takano-Murakami et al., 2009) a large number of individuals were diagnosed with SANFH after having suffered atypical pneumonia. Its etiology is currently a focus of research in this field, with many researchers having attempted to develop animal models of human SANFH. Mature among these efforts is the hormone + endotoxin-induced osteonecrosis rabbit model established by Yamamoto et al. (2007). Demonstrating similar histological changes to those observed in humans, the ability to be established in a short period of time (as rapidly as four weeks), and good repeatability, the animal model induced using this method is suitable for basic SANFH pathology research.

SANFH and osteocyte apoptosis

Also known as programmed cell death, apoptosis is caused by the triggering of an intracellular death program by internal and external factors. As an active mode of cell death, apoptosis is significantly different from necrosis in many respects. To date, many researchers have suggested that SANFH is closely associated with osteoblast and osteocyte apoptosis (Sato et al., 2001). Weinstein et al. (1998) discovered that administration of excess hormones can affect

the mechanism by which osteoblasts and osteoclasts are formed in bone marrow, decreasing the bone formation rate and mineral density, and inducing apoptosis of mature osteoblasts and osteocytes. Weinstein et al. (2000) suggested that the main role of hormones in this process is to induce apoptosis in osteoblasts and osteocytes, and decrease formation of osteoclasts, resulting in decreased bone turnover and continuous apoptosis, thus leading to femoral head necrosis.

Hormones have been widely accepted as an important cause of non-traumatic avascular necrosis of the femoral head. Moreover, experiments have confirmed that hormones induce apoptosis (Canalis and Delany, 2002). They not only promote apoptosis of osteoblasts and osteocytes, and decrease osteocyte numbers, but also affect osteoblast function, thereby delaying osteogenesis and mediating apoptosis, finally resulting in bone loss. The present study further clarified the role of apoptosis in SANFH.

Conflicts of interest

The authors declare no conflict of interest.

ACKNOWLEDGMENTS

Research supported by the National Science Foundation of China.

REFERENCES

Canalis E and Delany AM (2002). Mechanisms of glucocorticoid action in bone. *Ann. N. Y. Acad. Sci.* 966: 73-81.http://dx.doi.org/10.1111/j.1749-6632.2002.tb04204.x

Kerachian MA, Séguin C and Harvey EJ (2009). Glucocorticoids in osteonecrosis of the femoral head: a new understanding of the mechanisms of action. *J. Steroid Biochem. Mol. Biol.* 114: 121-128. http://dx.doi.org/10.1016/j.jsbmb.2009.02.007

Nishida K, Yamamoto T, Motomura G, Jingushi S, et al. (2008). Pitavastatin may reduce risk of steroid-induced osteonecrosis in rabbits: a preliminary histological study. *Clin. Orthop. Relat. Res.* 466: 1054-1058. http://dx.doi.org/10.1007/s11999-008-0189-4

Pietrogrande V (1955). [Hemopathy caused by osteopathy]. *Minerva Pediatr.* 7: 1652-1654.

Sato M, Sugano N, Ohzono K, Nomura S, et al. (2001). Apoptosis and expression of stress protein (ORP150, HO1) during development of ischaemic osteonecrosis in the rat. *J. Bone Joint Surg. Br.* 83: 751-759. http://dx.doi.org/10.1302/0301-620X.83B5.10801

Takano-Murakami R, Tokunaga K, Kondo N, Ito T, et al. (2009). Glucocorticoid inhibits bone regeneration after osteonecrosis of the femoral head in aged female rats. *Tohoku J. Exp. Med.* 217: 51-58. http://dx.doi.org/10.1620/tjem.217.51

Weinstein RS, Jilka RL, Parfitt AM and Manolagas SC (1998). Inhibition of osteoblastogenesis and promotion of apoptosis of osteoblasts and osteocytes by glucocorticoids. Potential mechanisms of their deleterious effects on bone. *J. Clin. Invest.* 102: 274-282. http://dx.doi.org/10.1172/JCI2799

Weinstein RS, Nicholas RW and Manolagas SC (2000). Apoptosis of osteocytes in glucocorticoid-induced osteonecrosis of the hip. *J. Clin. Endocrinol. Metab.* 85: 2907-2912.

Yamamoto T, Miyanishi K, Motomura G, Nishida K, et al. (2007). [Animal models for steroid-induced osteonecrosis]. *Clin. Calcium* 17: 879-886.

Yun SI, Yoon HY, Jeong SY and Chung YS (2009). Glucocorticoid induces apoptosis of osteoblast cells through the activation of glycogen synthase kinase 3beta. *J. Bone Miner. Metab.* 27: 140-148. http://dx.doi.org/10.1007/s00774-008-0019-5